iJRASET
International Journal For Research in Applied Science and Engineering Technology

INTERNATIONAL JOURNAL FOR RESEARCH

IN APPLIED SCIENCE & ENGINEERING TECHNOLOGY

Volume: 13 **Issue:** V **Month of publication:** May 2025

DOI: https://doi.org/10.22214/ijraset.2025.71592

www.ijraset.com

Call: 08813907089 | E-mail ID: ijraset@gmail.com

International Journal for Research in Applied Science & Engineering Technology (IJRASET)
ISSN: 2321-9653; IC Value: 45.98; SJ Impact Factor: 7.538
Volume 13 Issue V May 2025- Available at www.ijraset.com

Tailoring ZnO Emission for UV Devices: Enhanced Photoluminescence through Thiophenol Surface Capping

Shashi Bhushan Rana
Dept. of Engineering & Technology, Guru Nanak Dev University Regional Campus, Gurdaspur (Punjab)

Abstract: ***In this research, the optical characteristics of ZnO nanoparticles modified with 4-aminothiophenol were thoroughly examined. The surface modification was achieved through colloidal synthesis, employing a wet chemical precipitation method with carefully selected precursors.***
The attachment of 4-aminothiophenol molecules to the ZnO nanoparticle surfaces resulted in significant changes to their optical behaviour. These surface-modified nanoparticles were characterized using X-ray diffraction (XRD), scanning electron microscopy (SEM), and Fourier-transform infrared (FTIR) spectroscopy. Optical analysis was conducted using UV-Visible absorption and photoluminescence (PL) spectroscopy.
The study focused on understanding the underlying mechanisms behind the observed changes in fluorescence and absorption properties. Notably, the surface capping led to a marked enhancement of near-band-edge ultraviolet (UV) emission and a significant suppression of the defect-related green luminescence in the PL spectra. This enhancement indicates that surface defects, such as oxygen vacancies, were effectively passivated by the capping agent. The improved optical performance highlights the potential of these modified ZnO nanoparticles for advanced optoelectronic applications, including UV lasers and LEDs. Overall, the use of 4-aminothiophenol as a capping agent was shown to play a critical role in tuning the optical properties of ZnO nanoparticles.
Keywords: ZnO nanoparticles, PL, UV-Visible, XRD, SEM, oxygen vacancies, capping agent.

I. INTRODUCTION

Group II–VI compound semiconductor nanoparticles have attracted significant research attention due to their exceptional optical and electronic characteristics, largely attributed to quantum confinement effects and a high surface-to-volume ratio [1-3]. These properties have enabled their use in diverse optoelectronic applications, including light-emitting diodes, fluorescent lighting, display technologies, bio-imaging, and catalysis.

Researchers have focused on synthesizing nanoparticles with controlled structural attributes such as size, morphology, and crystallinity, often by engineering the nanoparticle surface [4-7]. The high surface-to-volume ratio implies a substantial number of atoms are located at the surface, leading to the presence of numerous surface electronic states that greatly influence the physical and optoelectronic behaviour of the nanoparticles [8-12].

One effective strategy for tailoring these surface states involves the use of capping agents—organic molecules that bind to the nanoparticle surface—allowing precise control over particle growth and surface chemistry [13-15]. In the present study, ZnO nanoparticles were synthesized using selected chemical precursors, followed by surface modification with 4-aminothiophenol as a capping agent. Zinc oxide (ZnO) is a widely favoured material for such applications due to its wide direct bandgap of 3.37 eV, which supports operation at high voltages, and its large exciton binding energy (60 meV), which enables efficient exciton recombination at room temperature [16-19]. These features make ZnO highly suitable for optoelectronic applications such as UV lasers, sensors, and display devices. The optical performance of ZnO can also be fine-tuned by altering the nanoparticle size, which affects its luminescent properties. Several synthesis techniques have been explored for producing ZnO nanoparticles, including sol-gel processing, chemical vapor deposition, micro-emulsion, spray pyrolysis, and wet chemical precipitation [20-22]. Among these, the wet chemical method stands out for its simplicity, cost-effectiveness, and ability to yield homogeneous mixtures at the molecular level, ensuring better control over particle morphology, stoichiometry, and purity. However, achieving high-quality ZnO nanoparticles with optimal optical properties requires careful attention to minimizing structural defects, which can otherwise lead to particle aggregation and reduced luminescence performance [23-25].

Photoluminescence (PL) spectra of ZnO nanoparticles typically exhibit a strong UV emission due to excitonic recombination and a broad visible emission arising from various intrinsic defects, including zinc interstitials, zinc vacancies, and most notably, oxygen vacancies. These surface-related defects significantly impact the visible emission observed in PL spectra.

Previous studies, such as that by van Dijken et al., have emphasized the crucial role of surface states in governing defect-related emissions. While various capping agents like polyvinylpyrrolidone (PVP), polyvinyl butyral (PVB), and PMMA have been employed to mitigate these emissions, none have fully suppressed the visible luminescence associated with defects [26-29].

In this work, 4-aminothiophenol was employed as a novel capping agent, leading to a notable enhancement of UV emission and near-complete suppression of visible defect-related luminescence in the PL spectra. This molecule demonstrated a threefold advantage: it effectively binds to the ZnO nanoparticle surface, thereby maintaining a minimal particle size; it prevents nanoparticle agglomeration through steric hindrance; and it passivates surface defects that would otherwise contribute to non-radiative recombination pathways.

As a result, this capping approach offers significant potential for optimizing ZnO nanoparticles for high-performance optoelectronic applications.

II. EXPERIMENTAL SECTION

A. *Synthesis of Surface-Modified ZnO Nanoparticles Using 4-Aminothiophenol*

All reagents used in this study were procured from Sigma-Aldrich with a certified purity of 99.999% and were utilized without any further purification. The synthesis of ZnO nanoparticles was carried out in a two-neck round-bottom flask by dissolving zinc nitrate hexahydrate [$Zn(NO_3)_2 \cdot 6H_2O$] (600 mg, 2.0 mmol) and 4-aminothiophenol (600 mg, 4.0 mmol) in 30 mL of dry methanol. The solution was stirred continuously for 10 minutes at a constant temperature of 25°C under a nitrogen atmosphere to prevent oxidation of the 4-aminothiophenol.

Subsequently, a sodium hydroxide (NaOH) solution was introduced dropwise using a dropping funnel. The resulting mixture was subjected to ultrasonic treatment in a bath for three hours, promoting the formation of a stable dispersion of ZnO nanoparticles. The dispersion was then purified through repeated centrifugation, filtration, and washing with methanol and deionized water, typically four to five cycles. The final step involved annealing the surface-capped ZnO nanoparticles in a vacuum oven at 300°C, with annealing durations varying across samples: Sample A (6 hours), Sample B (7 hours), Sample C (8 hours), Sample D (9 hours), and Sample E (10 hours).

B. *Characterization of the Capped ZnO NPs*

To thoroughly examine the structural features of the capped ZnO nanoparticles, X-ray diffraction (XRD) analysis was conducted using a PANalytical X'PERT PRO diffractometer, operated at 50 kV and 40 mA. The instrument employed nickel-filtered Cu Kα radiation (λ = 1.5406 Å) and recorded diffraction patterns within a 2θ range of 10° to 100°, with fine angular steps. Surface morphology was investigated using a JEOL JSM-6610LV scanning electron microscope (SEM) at an accelerating voltage of 10 kV. For SEM analysis, the nanoparticle samples were dispersed in ethanol to prepare suitable specimens.

Photoluminescence (PL) properties were evaluated with a Perkin Elmer LS 45 luminescence spectrometer, using a 325 nm excitation wavelength. A xenon lamp with a power equivalent to 1000 kW and a 5 ms pulse duration served as the excitation source, and all measurements were carried out at room temperature. Ultraviolet-visible (UV-Vis) absorption spectra were recorded on a Specord 250 Plus Analytik Jena spectrophotometer. Fourier-transform infrared (FTIR) spectroscopy was performed using a Bruker Tensor 27 spectrometer over the spectral range of 600–4000 cm^{-1} to identify functional groups and confirm surface modification. For comparative analysis, uncapped ZnO nanoparticles were also synthesized using similar precursors and procedures in the initial phase of the study.

III. RESULTS AND DISCUSSION

A key objective of this study was to analyze and present the results obtained from various characterization techniques applied to ZnO nanoparticles capped with 4-aminothiophenol. For a comprehensive comparison, corresponding data for uncapped ZnO nanoparticles subjected to identical annealing durations were also included. This parallel approach allowed for a clear evaluation of the differences in structural and optical properties between the capped and uncapped ZnO nanoparticles, highlighting the impact of surface modification through capping.

A. X-ray diffraction (XRD) of uncapped and capped ZnO nanoparticles

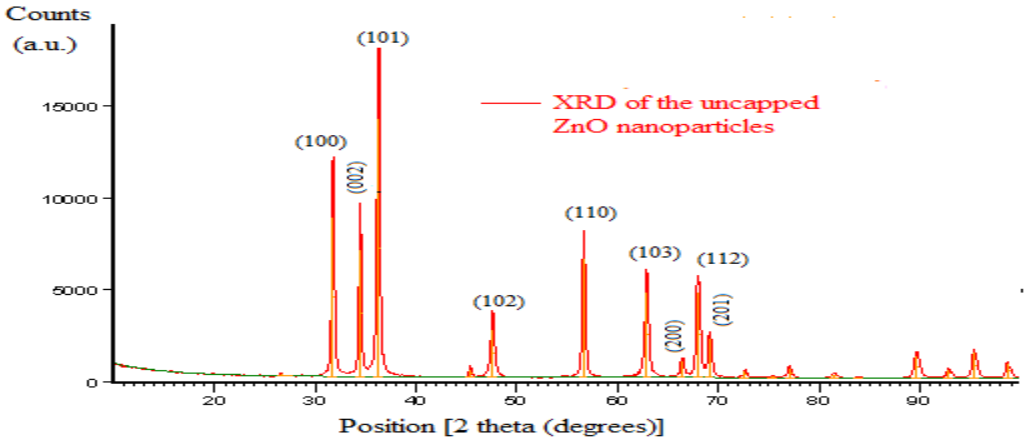

Fig.1 XRD of the uncapped ZnO nanoparticles

In this study, the crystallite sizes of uncapped and 4-aminothiophenol-capped ZnO nanoparticles were compared using X-ray diffraction (XRD) analysis. The XRD pattern of the uncapped ZnO nanoparticles, illustrated in Fig. 1, reveals well-defined diffraction peaks corresponding to the (100), (002), (101), (102), (110), (103), (200), (112), and (201) crystal planes. These peaks appear at 2θ values of 31.75°, 34.38°, 36.22°, 47.32°, 56.34°, 62.72°, 66.22°, 67.52°, and 68.1°, respectively, confirming the formation of a crystalline wurtzite structure. The crystallite sizes were determined using the Debye-Scherrer equation: $D = 0.9\lambda/(B\cos\theta)$

where D represents the average crystallite diameter, λ is the X-ray wavelength of Cu Kα radiation, B is the full width at half maximum (FWHM) of the selected peak, and θ is the Bragg angle. Based on this formula, the calculated average crystallite size for the uncapped ZnO nanoparticles was approximately 34 nm.

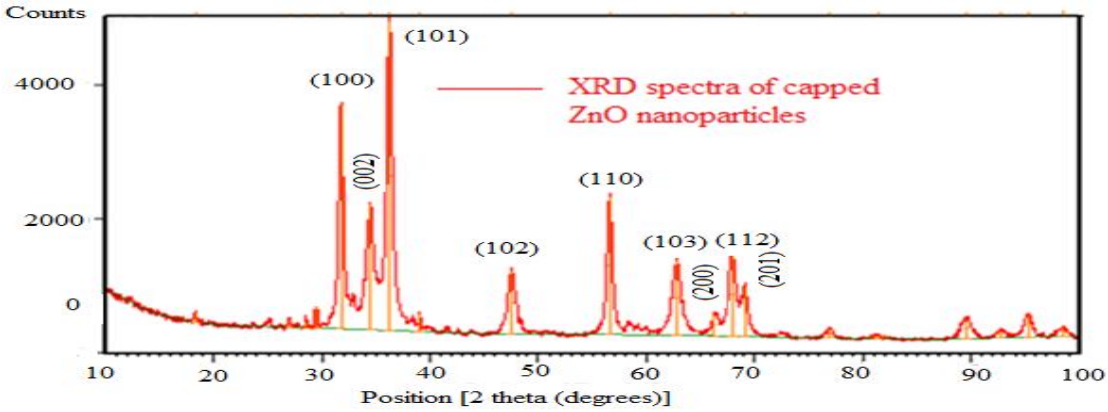

Fig.2 XRD spectra of the capped ZnO nanoparticles (4-aminothiophenol)

Figure 2 presents the XRD pattern of ZnO nanoparticles surface-modified with 4-aminothiophenol. The diffraction peaks of the capped samples are indexed to planes including (100), (002), (101), (102), (110), (103), (200), (112), and (201), which align well with the hexagonal wurtzite phase of ZnO, as referenced by the standard JCPDS card No. 36-1451. The observed peak positions and interplanar spacing confirm the formation of a stable wurtzite crystal structure in the capped nanoparticles.

In this analysis, we specifically considered Sample A, which underwent annealing for six hours in the colloidal phase. Compared to the uncapped nanoparticles, the capped samples displayed noticeably broader XRD peaks. This broadening is indicative of a reduced crystallite size, which was estimated to be approximately 21 nm using the Debye-Scherrer equation. The absence of additional peaks in the XRD spectrum suggests that the synthesized capped ZnO nanoparticles are free from secondary phases or impurities, underscoring their high purity.

Furthermore, although peak broadening is evident due to capping, the primary diffraction peaks remain consistent with the hexagonal wurtzite structure. This demonstrates that surface modification with 4-aminothiophenol does not disrupt the intrinsic crystal structure of the ZnO nanoparticles, while effectively reducing particle size.

B. Morphology of the uncapped and capped ZnO nanoparticles (SEM study)

Scanning Electron Microscopy (SEM) was employed to analyze the surface topography and morphology of the ZnO nanoparticles, offering valuable insights into their shape, size, and growth characteristics. Figure 3 displays the SEM image of the uncapped ZnO nanoparticles, revealing a relatively uniform structure with an average grain size of approximately 92 nm. These particles appear agglomerated, likely due to the inherently high surface energy of individual ZnO nanoparticles, and no secondary phases are observed.

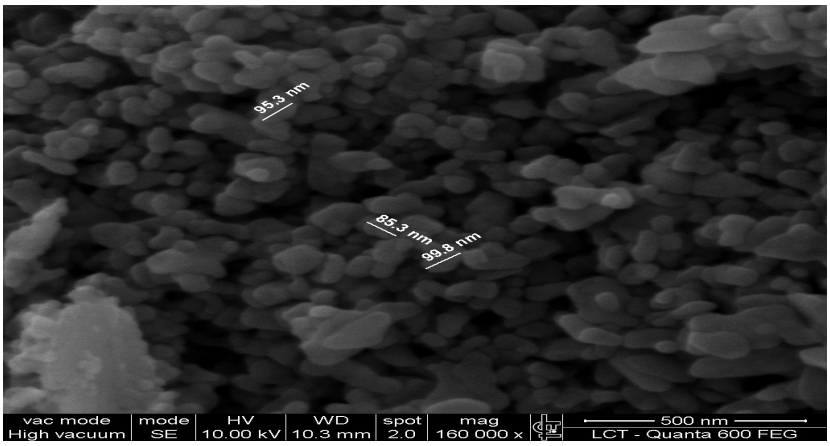

Fig. 3 SEM image of the uncapped ZnO nanoparticles

In contrast, Figure 4 presents the SEM micrograph of capped ZnO nanoparticles from Sample A, which was annealed for six hours in a colloidal medium. This image shows well-separated, irregularly shaped particles with significantly reduced agglomeration and an average grain size of about 57 nm. The reduced clustering demonstrates the effectiveness of 4-aminothiophenol in preventing nanoparticle aggregation through surface passivation.

It is important to note that the grain size values obtained from SEM and XRD analyses differ. This variation arises because SEM measures the physical size of particles based on visible grain boundaries, while XRD estimates crystallite size based on the coherent diffraction domains that scatter X-rays. As a result, XRD typically yields smaller size values, reflecting only the crystalline portion of the particles.

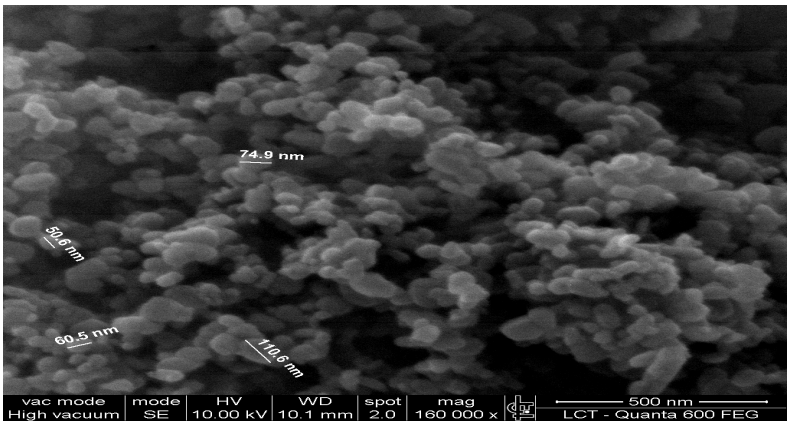

Fig.4 SEM image of the capped ZnO nanoparticles (4-aminothiophenol)

Additionally, the SEM image reveals that the capped ZnO nanoparticles are well dispersed and predominantly spherical in shape. A noticeable shadow-like region surrounding the particles suggests the presence of the organic capping layer, confirming successful surface modification with 4-aminothiophenol.

C. Photoluminescence (PL) investigation of uncapped and capped ZnO nanoparticles with 4-aminothiophenol

To investigate the emission characteristics of ZnO nanoparticles, photoluminescence (PL) spectroscopy was conducted on both uncapped and 4-aminothiophenol-capped ZnO samples. Figure 5 illustrates the PL spectrum of the uncapped ZnO nanoparticles synthesized from high-purity precursors. A prominent peak at 377 nm corresponds to near-band-edge (NBE) ultraviolet (UV) emission, commonly attributed to excitonic recombination in ZnO [26–27]. In contrast, the broader emission range from 444 nm to 542 nm represents defect-related visible luminescence.

Specifically, the peak at 444 nm is associated with blue emission, 459 nm with weak blue-green, 484 nm with intense blue-green, and the broad band from 484 nm to 542 nm corresponds to green emission. These emissions arise from intrinsic defects such as interstitial zinc atoms and the presence of donor and acceptor states located between the valence and conduction bands [28]. The green emission, in particular, is linked to singly ionized oxygen vacancies on the surface of ZnO nanoparticles.

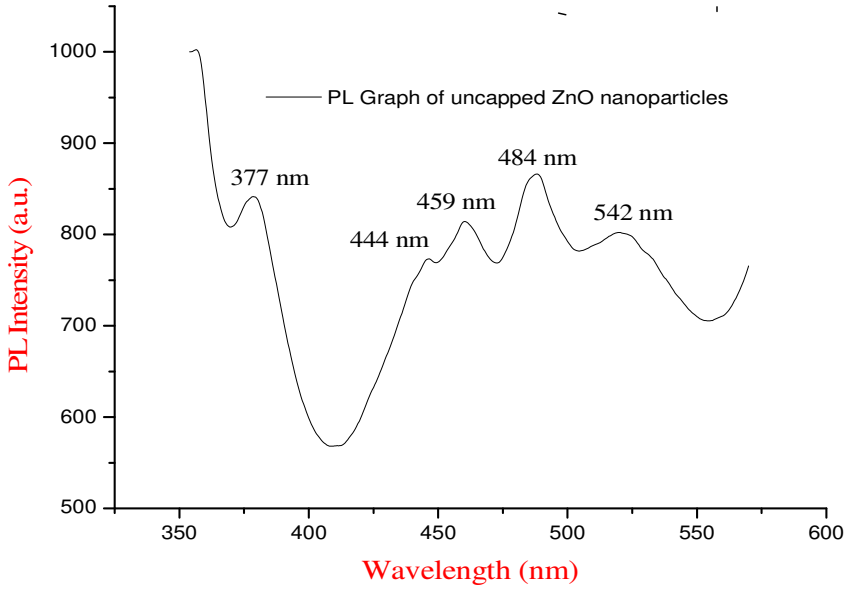

Fig. 5 PL spectra of the uncapped ZnO nanoparticles

Upon excitation with 325 nm UV light from a xenon lamp, uncapped ZnO nanoparticles exhibit both strong visible and moderate UV emission. This pronounced visible luminescence is primarily due to a high density of surface defects, which is a consequence of their high surface-to-volume ratio. As nanoparticle size decreases, the number of surface states increases, leading to enhanced defect-related emissions.

Surface modification with 4-aminothiophenol significantly alters the PL behaviour. When the capped ZnO nanoparticles (Sample A) were excited at 325 nm under room temperature conditions, a marked suppression of visible emission was observed alongside an enhancement in UV luminescence. This enhancement is attributed to the reduction of non-radiative surface defects caused by effective passivation from the capping agent.

Surface modification of ZnO nanoparticles using the capping agent 4-aminothiophenol leads to a near-complete suppression of photoluminescence in the visible region. As depicted in Fig.6, the capped ZnO nanoparticles exhibit a prominent UV emission peak centred around 345 nm, indicating their potential use in ultraviolet light-emitting applications. We investigated the impact of varying the reflux duration on the photoluminescence (PL) intensity. Refluxing was carried out at 300°C, with durations incremented hourly across five samples: 6, 7, 8, 9, and 10 hours. The PL intensity showed a consistent increase with longer reflux times. This enhancement in PL intensity correlates with an increase in the nanoparticle size, which occurs as the reflux time extends. At the shortest reflux time (6 hours), the nanoparticles are smallest, yielding the lowest PL intensity. Conversely, the longest reflux time (10 hours) produces the largest nanoparticles and the highest PL intensity, as illustrated in Fig.6.

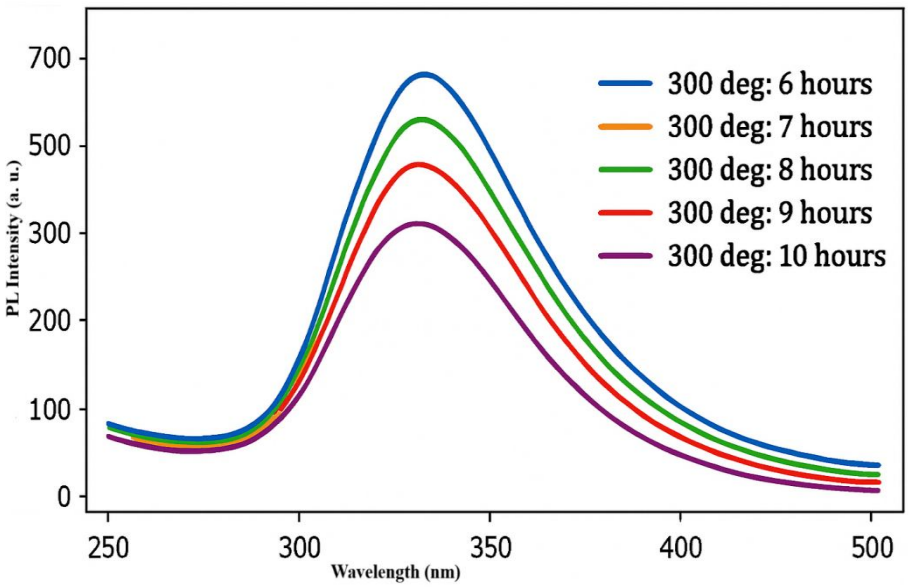

Fig. 6 PL spectra of the capped ZnO nanoparticles at different annealing (reflux)times

Therefore, surface passivation through capping effectively mitigates these recombination centres, improving the quantum efficiency of ZnO-based nanostructures. The PL results confirm that surface modification not only suppresses defect-related visible emission but also promotes stronger UV emission, enhancing the optical quality of ZnO nanoparticles for use in optoelectronic applications.

D. UV-Visible Absorption Analysis of Uncapped and Capped ZnO Nanoparticles

The optical behaviour of ZnO nanoparticles becomes increasingly significant as their size is reduced to the nanoscale. A comparative UV-Visible absorption analysis was conducted for both uncapped and 4-aminothiophenol-capped ZnO nanoparticles. As illustrated in Fig. 7, the absorption spectrum of the uncapped ZnO nanoparticles shows a peak near 375 nm, indicative of excitonic absorption caused by the strong exciton binding energy characteristic of ZnO at ambient temperature. This absorption peak at 375 nm also demonstrates a slight blue shift compared to the bulk ZnO absorption edge at 377 nm, a shift attributed to quantum confinement effects within the nanoparticles.

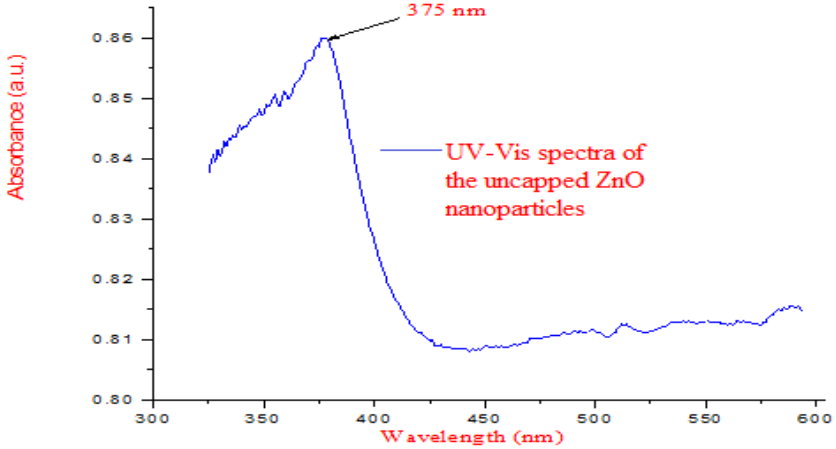

Fig.7 UV-Visible absorption spectra of the uncapped ZnO nanoparticles

Subsequently, we analysed the absorption characteristics of ZnO nanoparticles capped with 4-aminothiophenol. These capped samples were annealed in a colloidal solution at 300ºC for varying durations of 6, 7, 8, 9, and 10 hours and designated as Samples A through E.

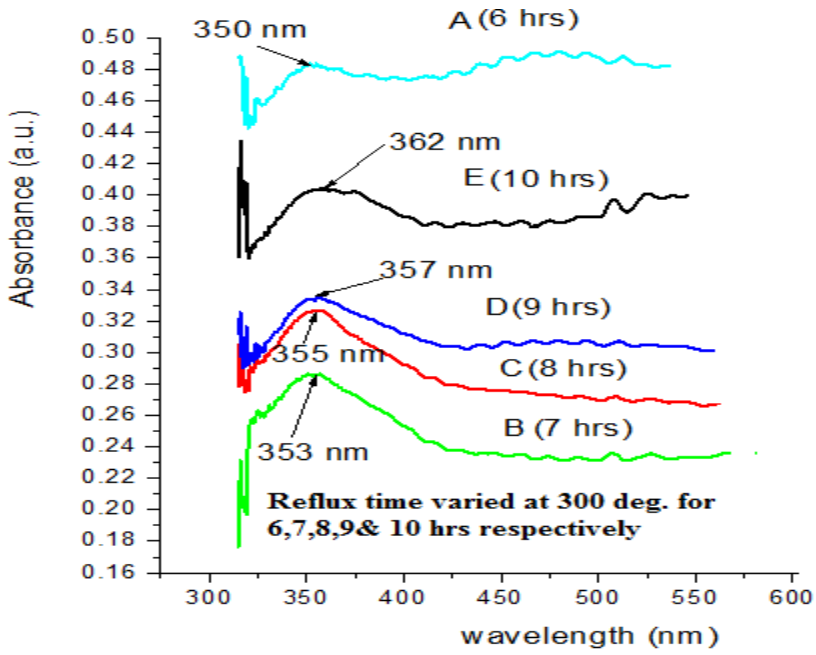

Fig.8 UV-visible absorption spectra of the capped ZnO nanoparticles

Previous literature indicates that an absorption wavelength of 377 nm (corresponding to a band gap energy of 3.28 eV) is typical for bulk ZnO [37]. In our experiments, the UV-Visible absorption spectra of the capped nanoparticles, shown in Fig. 8, lie in the range of 350 nm to 362 nm, depending on the reflux duration. The progressive blue shift in absorption from 373 nm down to 350 nm is again a result of quantum confinement effects in the smaller nanoparticles.

As reflux time increased from 6 to 10 hours, the absorption edge gradually shifted toward longer wavelengths (red shift), indicating an increase in nanoparticle size. This red shift, from 350 nm to 362 nm, suggests that the nanoparticles grow in size with prolonged refluxing at 300ºC. Thus, the smallest nanoparticles (Sample A, 6 hours) absorbed at 350 nm, while the largest ones (Sample E, 10 hours) showed maximum absorption at 362 nm.

The direct correlation between reflux time and particle size also influences the band gap energy, calculated using the equation ($E_g = hc/\lambda$) using this formula, the band gap narrows with increasing reflux time comes out to be 3.54 eV at 6 hours to 3.42 eV at 10 hours. This trend further confirms the size-dependent optical properties of capped ZnO nanoparticles.

IV. CONCLUSIONS

Capped ZnO nanoparticles were successfully synthesized using the wet chemical precipitation method, with 4-aminothiophenol employed as the capping agent. Their optical characteristics were explored through both photoluminescence and UV-Visible absorption spectroscopy. The photoluminescence results clearly demonstrated the impact of the capping process, with a significant suppression of defect-related visible emissions and a marked enhancement in ultraviolet emission intensity. Additionally, UV-Visible absorption spectra revealed a noticeable blue shift in the absorption edge for the capped nanoparticles compared to their uncapped counterparts. This shift is attributed to the quantum confinement effect, which indicates that the capped ZnO nanoparticles are smaller in size and absorb light at shorter wavelengths than the uncapped ones. These observations confirm the effectiveness of the capping agent in tailoring both the emission and absorption properties of ZnO nanoparticles at the nanoscale.

REFERENCES

[1] U. Ozgur, Ya. I. Alivov, C. Liu, A. Teke, M.A. Reshchikov, S. Dogan, V. Avrutin, S.J. Cho, H. Morkoc, Appl. Phys. Rev., J. Appl. Phys. 98 (2005) 041301.
[2] S. Liang, H. Sheng, Y. Liu, Z. Hio, Y. Lu, H. Shen, J. Cryst. Growth 225 (2001) 110.
[3] N. Saito, H. Haneda, T. Sekiguchi, N. Ohashi, I. Sakagushi, K. Koumoto, Adv. Mater. 14 (2002) 418.
[4] H. Kim, A. Pique, J.S. Horwitz, H. Murata, Z.H. Kafafi, C.M. Gilmore, D.B. Chrisey, Thin Solid Films 377 (2000) 798.
[5] F. Meng, J. Yin, Y.Q. Duan, Z.H. Yuan, L.J. Bie, Sensors Actuators B 156 (2011) 703.
[6] Z. Liu, C. Liu, J. Ya, E. Lei, Renew. Energy 36 (2011) 1177.
[7] E. Tang, G. Cheng, X. Ma, X. Pang, Q. Zhao, Appl. Surf. Sci. 252 (2006) 5227.
[8] V. A. L. Roy, A. B. Djurisic, W. K. Chan, J. Cao, H. F. Lui, C. Surya, Applied Physics Letters 83 (2003) 141.

[9] X. Du, Y. Fu, J. Sun, X. Han, J. Liu, Semicond. Sci. Technol. 21 (2006) 1202.
[10] F. Grasset et al., J. Alloys Comp. 360 (2003) 298.
[11] R. Elilarassi, G. Chandrasekaran, Optoelectron. Lett. 6 (2010) 6.
[12] S. Suwanboon, P. Amornpitoksuk, P. Bangrak, Ceram. Int. 37 (2011) 333.
[13] H. Liu, J. Yang, Z. Hua, Y. Zhang, L. Yang, L. Xiao, Z. Xie, Appl. Surf. Sci. 256 (2010) 4162.
[14] N.R. Yogamalar, A.C. Bose, J. Solid State Chem. 184 (2011) 12.
[15] T. Sahoo, M. Kim, J.H. Baek, S.R. Jeon, J.S. Kim, Y.T. Yu, C.R. Lee, I.H. Lee, Mater. Res. Bull. 46 (2011) 525.
[16] Y. H. Tong, Y. C. Liu, S.X. Lu, L. Dong, S. J. Chen, Z. Y. Xiao, Journal of Sol-Gel Science and Technology 30 (2004) 157.
[17] L. Guo, S. Yang, C. Yang, P. Yu, J. Wang, W. Ge, G.K.L. Wong, Chemistry of Materials 12 (2000) 2268.
[18] Zhuang Jia, Liu Mang and Liu Hanbin, Sci. China Ser B-Chem 52 (2009) 2125.
[19] R.Y. Hong, J. Z. Qian, J. X. Cao, Powder Technology 163 (2006) 160.
[20] X. Peng, L. Manna, W. Yang, J. Wickham, E. Scher, A. Kadavanich, A.P. Alivisatos, Nature 404 (2000) 59.
[21] Y. L. Wu, A. I. Y. Tok, F. Y. C. Boey, X. T. Zeng, X. H. Zhang, Applied Surface Science 253 (2007) 5473.
[22] J. Wang and L. Gao, Solid State Commun. 132 (2004) 269.
[23] S. Maensiri, C.P. Laokul, V. Promarak, J. Cryst. Growth 289 (2006) 102.
[24] K. Pato, E. Swatsitang, W. Jareonboon, S. Maensiri, V. Promarak, Optoelectron. Adv. Mater. Rapid Commun. 1 (2007) 287.
[25] S. Maensiri, C. Masingboon, V. Promarak, S. Seraphin, Opt. Mater. 29 (2007) 1700.
[26] P. Erhart, K. Albe, A. Klein, Phys. Rev. B 73 (2006) 205203.
[27] A. Janotti, C.G. Van de Walle, Appl. Phys. Lett. 87 (2005) 122102.
[28] H. Zhang, D. Yang, S. Li, X. Ma, Y. Ji, D. Qu, Mater. Lett. 59 (2005) 1696.
[29] D.C. Aggarwal, Nucl. Instrum. Methods Phys. Res. B 244 (2006) 136.

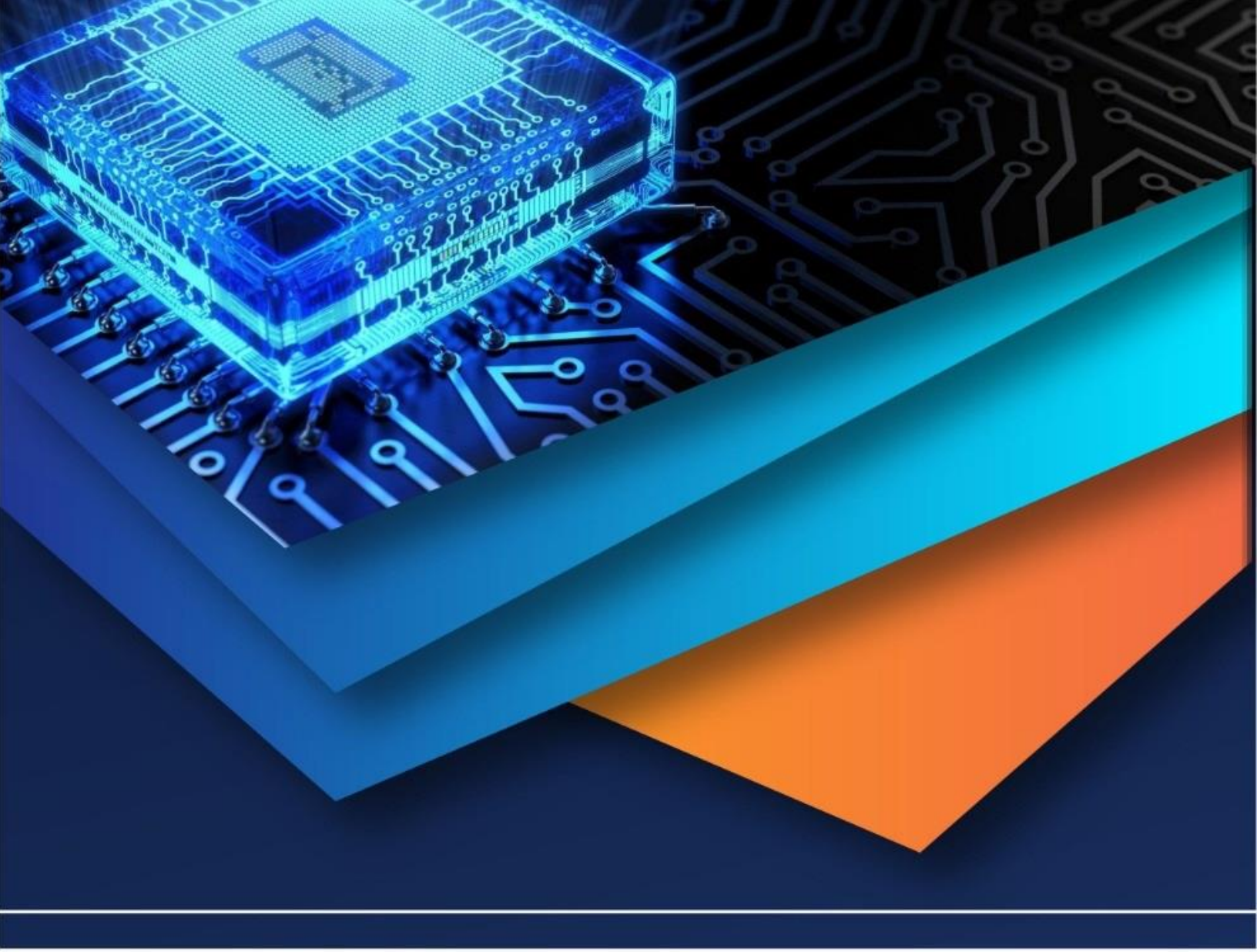

10.22214/IJRASET

45.98

IMPACT FACTOR: 7.129

IMPACT FACTOR: 7.429

INTERNATIONAL JOURNAL FOR RESEARCH

IN APPLIED SCIENCE & ENGINEERING TECHNOLOGY